
[View Journal Online](#)
[View Article Online](#)

Synthesis, crystal structure and *in vitro* anticancer studies of two *bis*(8-quinolinolato-N,O)-platinum(II) complexes

 Hong Chen ^{1,2} and Mingguo Liu ^{2,*}
¹ Key Laboratory of Radiation Physics and Technology of Ministry of Education, Institute of Nuclear Science and Technology, Sichuan University, Chengdu 610064, P. R. China

chenhong3041@126.com (H.C.)

² Hubei Key Laboratory of Natural Products Research and Development, College of Biological and Pharmaceutical Sciences, China Three Gorges University,

Yichang 443002, P. R. China

mglu1966@163.com (M.L.)

* Corresponding author at: Hubei Key Laboratory of Natural Products Research and Development, College of Biological and Pharmaceutical Sciences, China Three Gorges University, Yichang 443002, P. R. China.

 Tel: +86.717.6395580 Fax: +86.717.6395580 e-mail: mglu1966@163.com (M. Liu).

RESEARCH ARTICLE



doi: 10.5155/eurjchem.10.1.37-44.1814

Received: 06 November 2018

Received in revised form: 15 December 2018

Accepted: 18 December 2018

Published online: 31 March 2019

Printed: 31 March 2019

KEYWORDS

 DFT calculations
 Crystal structure
 Anticancer activity
 8-Hydroxyquinoline
 Platinum(II) complexes
 8-Hydroxy-2-methylquinoline

ABSTRACT

Two *bis*(8-quinolinolato-N,O)-platinum(II) complexes, C₁₈H₁₂N₂O₂Pt (1) and C₂₀H₁₆N₂O₂Pt (2), were synthesized and characterized by FT-IR, elementary analysis and X-ray single crystal diffraction. Complex 1 crystallizes in monoclinic, space group *P2₁/c* with *a* = 9.3413(7), *b* = 10.3893(9), *c* = 14.8495(12) Å, β = 100.574(7)°, *V* = 1416.7(2) Å³. Complex 2 crystallizes in monoclinic, space group *P2₁/n* with *a* = 9.5115(11), *b* = 15.5692(18), *c* = 16.720(2) Å, β = 94.544(2)°, *V* = 2468.3(5) Å³. Intermolecular C-H...O hydrogen bonding interactions, as well as Pt...Pt and π - π stacking interactions, help to stabilize the crystal structures. The preliminary *in vitro* anticancer activity of complexes 1 and 2 and the corresponding ligands (L1 and L2) were investigated using human cervical (Hela) and hepatocellular carcinoma (Hep-G2) cancer cell lines. The platinum(II) complexes can greatly inhibit the cell proliferation and show stronger cytotoxic activities against the tested cancer cell lines than both ligands.

 Cite this: *Eur. J. Chem.* 2019, 10(1), 37-44

 Journal website: www.eurjchem.com

1. Introduction

The application of inorganic chemistry to medicine is a rapidly developing field, and novel therapeutic and diagnostic metal complexes are now having an impact on medical practice. Advances in bio-coordination chemistry are crucial for improving the design of compounds to reduce toxic side effects and understand their mechanisms of action [1-4]. Among this, platinum-based anticancer agents are a mainstay of clinical drugs for the treatment of various solid tumors such as genitourinary, colorectal, and non-small cell lung cancers [5-9]. The leading anticancer drug, *cis*-platin, has been used for more than three decades in standard chemotherapy regimens either as a single therapeutic modality or in combination with other cytotoxic agents or radiotherapy [10-12]. However, the chemotherapy is associated with severe side effects because of intrinsic or acquired resistance and toxicity [13,14], which has motivated the inorganic chemists to find more effective, less toxic, and target-specific metal-based anticancer drugs [15]. Over the last 40 years, thousands of platinum complexes have

been prepared in the hope of finding new drugs with a more tolerable toxicological profile and higher efficacy [16]. These efforts have brought a series of drugs into clinical use, i.e. carboplatin, oxaliplatin, nedaplatin, lobaplatin, and heptaplatin (Figure 1), and about 10 other complexes are currently under clinical trials [17]. Inspired by the predecessor's excellent work [18-25], our laboratory is engaged in the search of discovering new types of platinum-based compounds and other organic anticancer compounds, not only for providing better anticancer drugs but also for mitigating the drawbacks [26-28]. In this paper, we report in detail the synthesis, crystal structure and antitumor activity *in vitro* of two *bis*(8-quinolinolato-N,O)-platinum(II) complexes.

2. Experimental

2.1. Materials and apparatuses

8-Hydroxyquinoline, 2-methyl-8-hydroxyquinoline and mitomycin were purchased from Sigma-Aldrich and used as received without further purification.

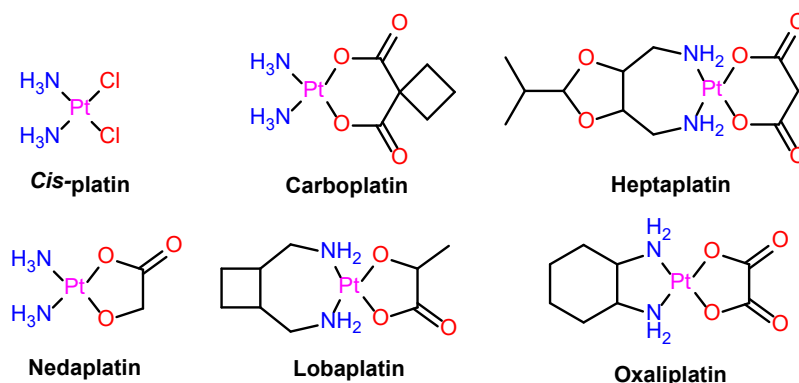
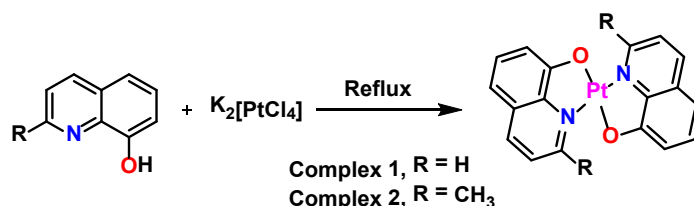


Figure 1. The structure of six platinum-based anticancer drugs.



Scheme 1. Synthetic procedure for complexes 1 and 2.

K₂[PtCl₄] was purchased from Alfa Aesar of 99.99% purity and the other starting materials were of analytical grade. Doubly distilled water was used to prepare the buffer solution. Dimethyl sulphoxide (DMSO) and cell culture reagents and media were purchased from Solarbio Beijing Ltd. FT-IR spectra were recorded on a PE-983 infrared spectrometer as KBr pellets with absorption in cm⁻¹. Elemental analysis (C, H, N) were taken on a Vario EL III elemental analysis instrument. Single-crystal X-ray diffraction data were collected on a SuperNova, Single source at offset, EOS diffractometer or Bruker APEX-II CCD diffractometer equipped with a graphite-monochromatic MoK α radiation ($\lambda = 0.71073 \text{ \AA}$).

2.2. Synthesis

Complexes 1 and 2 were synthesized according to the literature method reported by Scandola *et al.* [29,30], as depicted in Scheme 1. To an aqueous solution of K₂[PtCl₄] adjusted to ca pH = 10, two equimolar amounts of organic ligand (L1 or L2) were added and the solution heated to reflux for a few minutes. After cooling to room temperature, a dark-orange precipitate was deposited. This precipitate was recrystallized from dimethyl sulfoxide to give small red crystals of the title complexes. The filtrate of the reaction solution was allowed to stand for several days at room temperature to give more crystals. Then, the crystals were collected, washed with ethanol and dried in vacuum. Based on K₂[PtCl₄], the obtained yields of complexes 1 and 2 were 57 and 63%, respectively. The IR spectra of complex 1 revealed absorption bands at 1014 cm⁻¹ may probably due to the C-O or C-N group. The IR spectra of complex 2 revealed absorption bands at 1572 and 1485 cm⁻¹ may probably due to the C=C group.

Bis(8-Quinolinolato-N,O)-platinum(II) (1): Color: Red. Yield: 57% based on K₂[PtCl₄]. M.p.: 287-289 °C. Anal. calcd. for C₁₈H₁₂N₂O₂Pt: C, 44.73; H, 2.50; N, 5.80. Found: C, 44.56; H, 2.46; N, 5.66 %. FT-IR (KBr, ν , cm⁻¹): 2939 (w), 2893 (w), 1680 (vs), 1561 (vs), 1489 (s), 1456 (m), 1263 (m), 1127 (m), 1014 (s), 953 (m), 745 (s), 700 (m).

Bis(2-Methylquinolin-8-olato)-platinum(II) (2): Color: Red. Yield: 63%, based on K₂[PtCl₄]. M.p.: 298-300 °C. Anal. calcd. for C₂₀H₁₆N₂O₂Pt: C, 46.97; H, 3.15; N, 5.48. Found: C, 46.83; H, 3.27; N, 5.69 %. FT-IR (KBr, ν , cm⁻¹): 3106 (w), 2939 (w), 1710 (vs), 1572 (vs), 1485 (vs), 1465 (s), 1383 (m), 1214 (m), 1105 (s), 936 (s), 751 (s), 623 (m).

2.3. X-ray crystal structure determination of complexes 1 and 2

Crystals suitable for X-ray diffraction were obtained by successful selection of a single crystal from mostly tiny twin crystals and polycrystalline powder. A red single crystal of complex 1 with dimensions of 0.31×0.23×0.12 mm was selected and mounted on the top of a glass fiber. The data were collected by a SuperNova, Single source at offset, EOS diffractometer equipped with a graphite-monochromatic MoK α ($\lambda = 0.71073 \text{ \AA}$) radiation using a ω scan mode in the range of $3.0 \leq \theta \leq 26.4^\circ$ ($-11 \leq h \leq 10$, $-12 \leq k \leq 12$, $-18 \leq l \leq 18$) at 200.15 K. A total of 6148 reflections were collected, of which 2881 were independent ($R_{\text{int}} = 0.036$) and 2198 were observed with $I > 2\sigma(I)$. A red single crystal of complex 2 with dimensions of 0.22×0.20×0.18 mm was selected and mounted on the top of a glass fiber. The data were collected by a Bruker APEX-II CCD diffractometer equipped with a graphite-monochromatic MoK α ($\lambda = 0.71073 \text{ \AA}$) radiation using a ψ - ω scan mode in the range of $1.8 \leq \theta \leq 26.4^\circ$ ($-9 \leq h \leq 11$, $-18 \leq k \leq 19$, $-20 \leq l \leq 20$) at 296.15 K. A total of 14172 reflections were collected, of which 5025 were independent ($R_{\text{int}} = 0.035$) and 4153 were observed with $I > 2\sigma(I)$.

Using Olex2 [31], the two structures were solved with the ShelXS structure solution program using Patterson Methods and refined with the ShelXL refinement package using Least Squares minimization [32]. The non-hydrogen atoms were refined isotropically and all hydrogen atoms were positioned geometrically. For complex 1, the final $R = 0.030$, $wR = 0.069$ ($w = 1/[\sigma^2(F_o^2) + (0.0225P)^2]$, where $P = (Fo^2 + 2Fc^2)/3$), (Δ/σ)_{max} < 0.001, $S = 1.030$, ($\Delta\rho$)_{max} = 1.18 and ($\Delta\rho$)_{min} = -1.10 e/Å³. For complex 2, the final $R = 0.031$, $wR = 0.107$ ($w =$

$1/[\sigma^2(Fo^2) + (0.0623P)^2]$, where $P = (Fo^2 + 2Fc^2)/3$. $(\Delta/\sigma)_{\max} = 0.002$, $S = 1.130$, $(\Delta\rho)_{\max} = 1.58$ and $(\Delta\rho)_{\min} = -1.13 \text{ e}/\text{\AA}^3$.

2.4. Anticancer activity

The anti-proliferative effects were tested by MTT assay [33-36] in human cervical cancer cells (Hela) and hepatocellular carcinoma (Hep-G2). The cancer chemotherapeutic potential of mitomycin, Pt(II) complexes (**1** and **2**) and the corresponding ligands (**L1** and **L2**) were evaluated according to an established procedure [37]. Hela and Hep-G2 were purchased from the ATCC (American Type Culture Collection). These two cells were grown in 1640 medium under aseptic conditions, supplemented with 100 U/cm³ penicillin and 100 µg/cm³ streptomycin containing 10% (v:v) fetal bovine serum. All cells were grown at 37 °C in a cell culture incubator in the presence of 5% CO₂, relative humidity: 95%. According to the cell growth situation, the culture medium was exchanged every two days.

When the cell grew well, MTT assay could be carried out. The logarithmic phases of Hela and Hep-G2 were seeded at a density of 5×10^4 cells/cm³ into sterile 96-well flat-bottomed plates (CORNING, USA), and the side holes were filled with aseptic PBS buffer. Then the cells were placed in a 37 °C incubator with 5% CO₂. The test ligand (**L1** and **L2**) and mitomycin were dissolved in RPMI 1640 medium with the concentration of 1000 µmol/L and filtrated to remove bacteria by 0.22 µm separate film. Complex **1** (60.00 mg) or complex **2** (60.00 mg) was added to DMSO (500 µL) and centrifuged after sufficient oscillation. The supernatant was got and the precipitation was weighed after drying, then the concentration was calculated using difference method. After that, the solution was diluted into 1000 µmol/L with RPMI 1640 medium, then filtrated to remove bacteria by 0.22 µm separate film. Positive drug *cis*-platin solution was prepared with sterile saline into 1000 µmol/L as the mother liquor, and then diluted into the required concentration with complete RPMI 1640 medium. In each hole of the 96-well flat-bottomed plates, the highest content of DMSO was 0.2% (v:v). The four test compounds, *cis*-platin and mitomycin were diluted to 100 µmol/L before spotting with complete medium RPMI 1640. At the same time, the blank wells (medium, DMSO) were set. Each assay compound was carried out by using four replicates, and each compound solution (100 µL) was added to the replicate wells in the concentration of 100 µmol/L. Hela and Hep-G2 were incubated for 48 h. After that, 20 µL of MTT (5 mg/mL) was added. Four hours later, the supernatant of 96-well plates was carefully blotted, and the DMSO (150 µL) was added to solve the formazan produced [38,39]. Colorimetry was performed at the wavelength of 570 nm. Each hole absorbance (OD value) was determined, and the cell inhibition rate was calculated by using OD value averaged by four replicates. At the same time, the half inhibitory concentration (IC₅₀) was drawn. Experiment was repeated on at least three separate occasions. The survival rate is calculated as follows:

$$\text{Viability as control (\%)} = \frac{[\text{OD}_{\text{administration group}} - (\text{OD}_{\text{control}} - \text{OD}_{\text{DMSO}})]}{\text{OD}_{\text{control}}} \times 100\% \quad (1)$$

2.5. Statistical analysis

The data were expressed as means ± standard deviations [40]. The significance of difference was evaluated with one-way ANOVA, followed by the Student-Newman-Keuls or Games-Howell test by SPSS 13.0 software [41]. p-Values less than 0.05 were considered to be statistically significant.

2.6. Electronic structures calculations

The first-principles DFT calculations of five Pt(II) comp-

lexes were done using the Vienna ab-initio simulation package (VASP 5.2.2) [42-44] performing a variational solution of the Kohn-Sham equations in a plane-wave basis with energy cutoff of 300.0 eV. All atomic positions in the Pt(II) complexes were fully relaxed without symmetry restrictions in a fixed unit cell parameters using a conjugate-gradient algorithm. For modeling of complexes **1** and **2**, the unit cell parameters used were taken from the single crystal X-ray diffraction measurements. The unit cell parameters of other Pt(II) complexes were obtained from the Cambridge Crystallographic Data Centre via www.ccdc.cam.ac.uk/conts/retrieving.html. Electron exchange correlation interactions were treated using the generalized gradient approximation (GGA) as parameterized by Perdew, Burke and Ernzerhof (PBE) [45]. The electron ion interactions were described using the projector-augmented-wave (PAW) method [46]. The number of 10 valence electrons for each Pt ($5d^96s^1$), 6 for O atom ($2s^22p^4$) and 5 for N atom ($2s^22p^3$) were treated explicitly and the remaining core electrons together with the nuclei were described by PAW pseudopotentials.

To describe correctly the strong Coulomb repulsion (U) between the localized d electrons of Pt, the DFT + U approach, adding a Hubbard-like term to the effective potential was applied in all calculations as implemented in VASP package. In the present work, the approach described by Dudarev *et al.* [47] was applied, where an effective Hubbard parameter $U_{\text{eff}} = U - J$ enters the Hamiltonian, with U and J being the Coulomb (of 4 eV) and exchange interaction parameter (of 1 eV), respectively.

The density of states (DOS) of various Pt(II) complexes is shown in Figure 2. Band structure calculations for complexes **1** and **2** predicted gaps at the Fermi level of 1.63163 and 0.63302 eV, consistent with the magnitude and order of the experimental results. Band structure calculations for the other three Pt(II) complexes predicted gaps at the Fermi level of -0.29988, 1.90544 and 1.85686 eV, respectively.

3. Results and discussion

3.1. Crystal structure of complexes 1 and 2

Crystals of complexes **1** and **2** that suitable for single-crystal X-ray structure determination were obtained by recrystallization in the mixed solvent of dimethyl sulfoxide and ethanol. Both of the organic ligands are in a *trans* geometry in the crystal structure of complexes **1** and **2**. In the crystal structure of complex **1**, the molecule is essentially planar with a maximum deviation of 0.0046 Å for the Pt atom. As for complex **2**, the molecule is also essentially planar with a maximum deviation of -0.0071 Å for the Pt atom. Figure 3 and 4 show a perspective view of complexes **1** and **2** with atomic numbering. Figure 5 shows the fragment of the crystal packing structure in a unit cell. The crystallographic data, details of data collection and structure refinement parameters for complexes **1** and **2** are listed in Table 1. The hydrogen bond lengths and bond angles of complexes **1** and **2** are listed in Table 2.

Although the crystal structure of complex **1** has been reported by Masako Kato *et al.* [48] and Chi-Ming Che *et al.* [49], the lattice parameters described in this work are really different from the literature values. Complex **1** crystallized in the $P2_1/c$ space group of monoclinic system with $V = 1416.7(2) \text{ \AA}^3$, while it's $P2_1/n$ with $V = 703.0(3) \text{ \AA}^3$ in the literature report. It has a planar geometry with the molecules stacked in an inclined fashion with an interplanar spacing of 3.5111, 3.6042 and 3.6433 Å, revealing three kinds of weak intermolecular π - π stacking interactions [50] (Figure 5a and Table 3). The crystal structure display herringbone-like crystal packing arrangement, in which the molecules are held together in an edge-to-face orientation, and the intermolecular

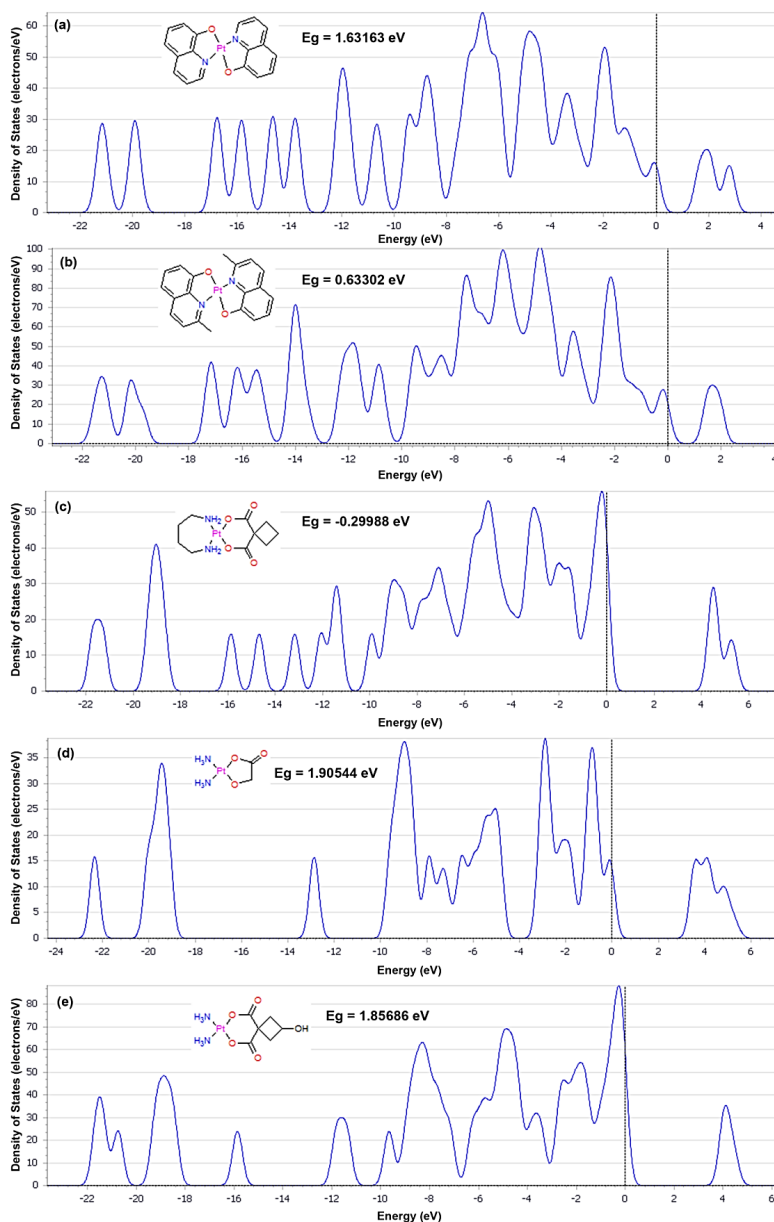


Figure 2. Density of states (DOS) for various Pt(II) complexes obtained by DFT calculation. The corresponding molecular structure and Fermi energy level were inserted in (a)-(e).

Pt...Pt distance is 3.8695(4) Å. The Pt atoms are four-coordinated planar by the N and O atoms from two 8-hydroxyquinoline, and the length of Pt(1)-O(1) (2.023(4) Å) and Pt(1)-O(2) (2.021(4) Å) is very close to the normal Pt-O coordination bond (2.01 Å) [51]. The angle of N(1)-Pt(1)-N(2) and N(1)-Pt(1)-O(1) is 179.03 and 82.15(18)°, respectively. Other selected bond length and bond angles are listed in Table 4.

Complex 2 crystallized in the $P2_1/n$ space group of monoclinic system with $V = 2468.3(5)$ Å³. The crystal structure of complex 2 determined in this work shows one and a half molecules in a dimeric form connected by weak intermolecular C-H...O hydrogen bonding interactions. The packing structure of complex 2 adopts a brick-wall-type face-to-face coplanar molecular arrangement with an interplanar separation of 3.3451(4) Å, thereby revealing the presence of intermolecular Pt...Pt short contacts (Figure 5b). The distance of π - π stacking between two 2-methyl-8-hydroxyquinoline rings is 3.5405 and 3.6794 Å (Table 3). The distance between

C(24) to the ring (Pt(1)-O(2)-C(19)-C(20)-N(2)) is 3.8615 Å, suggesting the existence of weak C-H... π stacking interactions. The length of Pt(1)-O(1) (2.016(5) Å) and Pt(2)-O(2) (2.015(5) Å) is very close to the normal Pt-O coordination bond (2.01 Å). The angle of N(1)-Pt(1)-N(2) and N(1)-Pt(1)-O(1) is 178.4(2) and 81.8(2)°, respectively. In each of the asymmetric unit, the planes of two molecular form dihedral angles of 87.24°.

3.2. Effects of complexes 1 and 2 on the anticancer activity

In this work, the anticancer effects of complexes 1 and 2, mitomycin and the ligands (L1 and L2) against two human cancer cells, cervical cancer (Hela) and carcinoma (Hep-G2), were investigated. Cell viability against drug concentrations was established, from which the IC₅₀ values were calculated, and this allows a direct comparison of the cytotoxicity of the complexes.

Table 1. Crystallographic data, details of data collection and structure refinement parameters for complexes **1** and **2**.

Complex	1	2
Empirical formula	C ₁₈ H ₁₂ N ₂ O ₂ Pt	1.5(C ₂₀ H ₁₆ N ₂ O ₂ Pt)
Formula weight (g.mol ⁻¹)	483.38	767.16
Crystal system	Monoclinic	Monoclinic
Space group	P2 ₁ /c	P2 ₁ /n
Morphology	Block	Block
Size (mm)	0.31×0.23×0.12	0.22×0.20×0.18
a (Å)	9.3413(7)	9.5115(11)
b (Å)	10.3893(9)	15.5692(18)
c (Å)	14.8495(12)	16.720(2)
α (°)	90.00	90.00
β (°)	100.574(7)	94.544(2)
γ (°)	90.00	90.00
V (Å ³)	1416.7(2)	2468.3(5)
Z	4	4
T (K)	200	296
D _c (g.cm ⁻³)	2.266	2.064
μ (mm ⁻¹)	9.916	8.543
F(000)	912.0	1464.0
Theta range for data collection (°)	1.7 ≤ θ ≤ 26.4	1.8 ≤ θ ≤ 26.4
h, k, l _{max}	11, 12, 18	11, 19, 20
Reflections collected / unique	6148/2881 [R _{int} =0.036]	14172/5025 [R _{int} =0.035]
Data/restraints/parameters	2881/0/208	5025/0/343
R indices (all data)	R ₁ =0.030, wR ₂ =0.069	R ₁ =0.031, wR ₂ =0.107
Largest diff. peak and hole (e Å ⁻³)	1.18 and -1.10	1.58 and -1.13
S (GOF on F ²)	1.03	1.13

Table 2. Hydrogen bond lengths (Å) and bond angles (°) of complexes **1** and **2**.

Complex	D-H...A	d(D-H)	d(H...A)	d(D...A)	∠ D-H...A
1	C(7)-H(7)···O(1) ⁱ	0.95	2.54	3.302(8)	137
	C(12)-H(12)···O(2) ⁱⁱ	0.95	2.59	3.446(8)	150
2	C11-H(11C)···O1	0.96	1.97	2.755(9)	137
	C1-H(1A)···O2	0.96	2.31	2.758(10)	107

Symmetry codes: (i) x, -y+1/2, z+1/2; (ii) -x+1, y+1/2, -z+1/2.

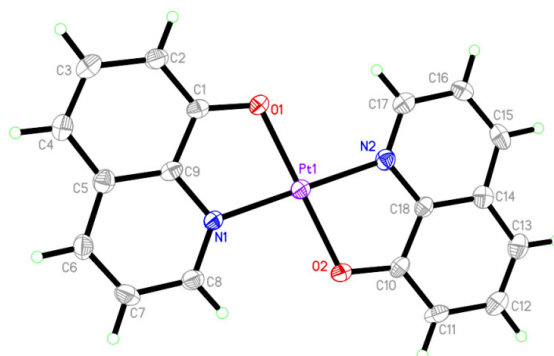
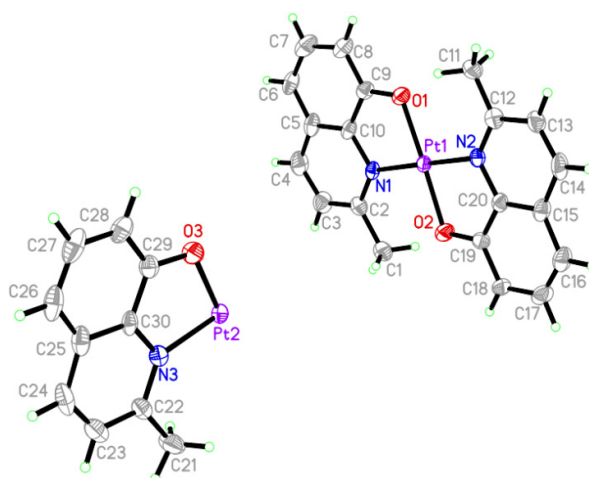
**Figure 3.** ORTEP drawing of the complex **1** with atom numbering scheme. Thermal ellipsoids for non-hydrogen atoms are drawn at the 35% probability level and H atoms are shown as small sphere.**Figure 4.** ORTEP drawing of the complex **2** with atom numbering scheme. Thermal ellipsoids for non-hydrogen atoms are drawn at the 35% probability level and H atoms are shown as small sphere.

Table 3. π - π Stacking Interactions in the crystal of complexes **1** and **2** (\AA , $^\circ$).

Complex	Cg(I) ... Cg(J)	Symmetry code	Cg-Cg (\AA)	Alpha ($^\circ$)
1	Cg(4) [1]...Cg(4)	$1-x, 1-y, -z$	3.5111	0
	Cg(5) [1]...Cg(3)	$-x, -y, -z$	3.6042	0.048
	Cg(5) [1]...Cg(5)	$-x, -y, -z$	3.6433	0
2	Cg(4) [1]...Cg(12)	$3/2-x, -1/2+y, 1/2-z$	3.5405	1.397
	Cg(3) [1]...Cg(12)	$1/2+x, 1/2-y, 1/2+z$	3.5696	4.472
	Cg(6) [1]...Cg(11)	$3/2-x, -1/2+y, 1/2-z$	3.5686	1.491
	Cg(11) [2]...Cg(5)	$-1/2+x, 1/2-y, -1/2+z$	3.6275	3.157

Complex 1: Cg(3): N1-C8-C7-C6-C5-C9; Cg(4): N2-C17-C16-C15-C14-C13; Cg(5): C1-C2-C3-C4-C5-C9. Complex 2: Cg(3): N1-C2-C3-C4-C5-C10; Cg(4): N2-C12-C13-C14-C15-C20; Cg(5): C5-C6-C7-C8-C9-C10; Cg(6): C15-C16-C17-C18-C19-C20; Cg(11): N3-C22-C23-C24-C25-C30; Cg(12): C25-C26-C27-C28-C29-C30.

Table 4. Selected bond lengths (\AA) and bond angles ($^\circ$) of complexes **1** and **2**.

Complex	Atom-Atom	Bond distance	Atom-Atom	Bond distance	Atom-Atom-Atom	Angle	
1	Pt(1)-O(1)	2.021(4)	Pt(1)-O(2)	2.024(4)	O(1)-Pt(1)-O(2)	179.03(17)	
	Pt(1)-N(1)	2.003(5)	Pt(1)-N(2)	2.004(5)	N(1)-Pt(1)-O(1)	82.51(18)	
	O(1)-C(1)	1.320(7)	O(2)-C(10)	1.324(7)	N(1)-Pt(1)-O(2)	97.49(18)	
	N(1)-C(8)	1.326(7)	N(1)-C(9)	1.373(7)	N(1)-Pt(1)-N(2)	179.6(2)	
	N(2)-C(17)	1.316(8)	N(2)-C(18)	1.371(7)	N(2)-Pt(1)-O(1)	97.85(18)	
	C(1)-C(2)	1.361(8)	C(1)-C(9)	1.430(8)	C(8)-N(1)-Pt(1)	128.7(4)	
	C(2)-C(3)	1.405(9)	C(3)-C(4)	1.379(9)	C(8)-N(1)-C(9)	120.0(5)	
	C(4)-C(5)	1.402(9)	C(5)-C(6)	1.422(9)	C(9)-N(1)-Pt(1)	111.3(4)	
	C(5)-C(9)	1.417(9)	C(6)-C(7)	1.361(9)	C(17)-N(2)-C(18)	119.8(5)	
	C(10)-C(11)	1.365(8)	C(10)-C(18)	1.433(8)	O(1)-C(1)-C(2)	125.7(6)	
	2	Pt(1)-O(1)	2.015(5)	Pt(1)-O(2)	2.016(5)	O(1)-Pt(1)-O(2)	177.9(2)
		Pt(1)-N(2)	2.051(5)	Pt(10)-N(1)	2.037(6)	O(1)-Pt(1)-N(2)	98.4(2)
		Pt(2)-O(3)	2.007(5)	Pt(2)-O(3) ⁱ	2.007(5)	O(1)-Pt(1)-N(1)	81.9(2)
Pt(2)-N(3)		2.051(6)	Pt(2)-N(3) ⁱ	2.051(6)	O(2)-Pt(1)-N(2)	81.8(2)	
O(1)-C(9)		1.314(9)	O(2)-C(19)	1.326(9)	O(2)-Pt(1)-N(1)	97.8(2)	
O(3)-C(29)		1.331(9)	N(2)-C(12)	1.304(9)	N(1)-Pt(1)-N(2)	178.4(2)	
N(2)-C(20)		1.384(9)	N(1)-C(2)	1.325(9)	O(3) ⁱ -Pt(2)-O(3)	180.00(1)	
N(1)-C(10)		1.396(9)	N(3)-C(22)	1.354(9)	O(3) ⁱ -Pt(2)-N(3)	98.7(2)	
N(3)-C(30)		1.374(9)	C(12)-C(11)	1.466(11)	O(3) ⁱ -Pt(2)-N(3) ⁱ	81.3(2)	
C(5)-C(4)		1.391(13)	C(5)-C(10)	1.386(10)	O(3)-Pt(2)-N(3) ⁱ	98.7(2)	

Symmetry code: (i) $-x+1, -y+1, -z+2$.

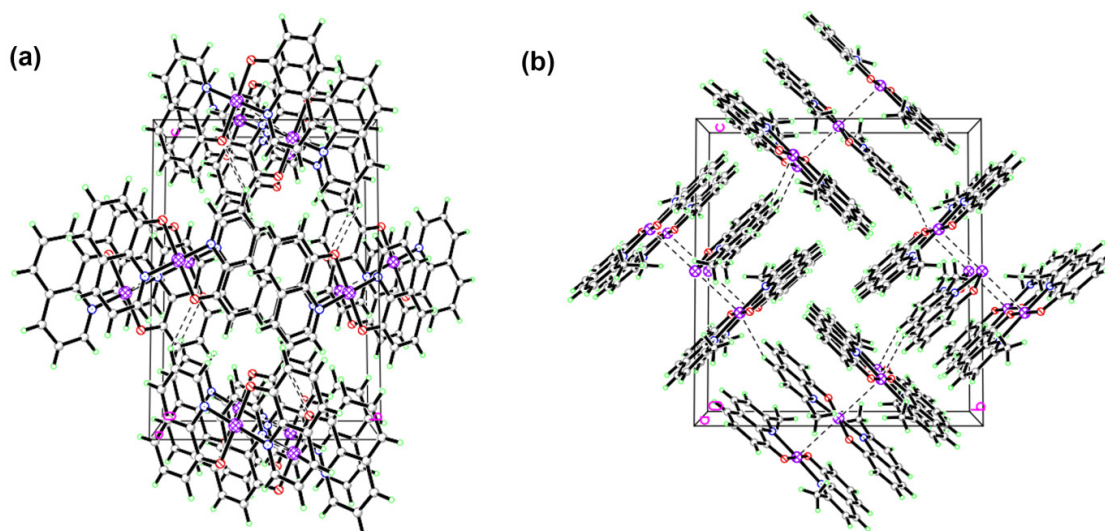


Figure 5. (a) Packing diagram of complex **1** in a unit cell viewed down the a direction. The dashed lines demonstrate the intermolecular C-H...O hydrogen bonding interactions; (b) Packing diagram of complex **2** in a unit cell viewed down the a direction. The dashed lines demonstrate the intermolecular Pt...Pt stacking and C-H...O hydrogen bonding interactions.

The IC_{50} value for each complex is presented in Table 5. The ligands (**L1** and **L2**) are capable of killing both cancer derived cell lines only at higher concentration with an IC_{50} value greater than 1000 $\mu\text{mol/L}$, thus are essentially inactive to inhibit cancer cells. When the ligands react with $K_2[PtCl_4]$, the resulting complexes **1** and **2** exhibit much better anticancer activity for both the Hep-G2 and Hela cell lines. For inhibition of the Hep-G2 cell, the IC_{50} of complexes **1** and **2** is 63.95 and 91.75 $\mu\text{mol/L}$, respectively, much lower than the ligands. For inhibition of the Hela cells, the IC_{50} is 57.39 and 73.45 $\mu\text{mol/L}$, also better than that of the ligands.

For both cancer cells, cisplatin or mitomycin has IC_{50} of about 10-20 $\mu\text{mol/L}$, showing very good inhibitory effect. The better anticancer effect of complexes **1** and **2** may be ascribed to the Pt(II) complex to have stronger DNA binding and cleavage and induce apoptosis in cancer cells [52-54]. However, further investigation on the anticancer mechanism is underway in our laboratory, and the ligand may be further improved for enhancing the anticancer activity of platinum complexes.

Table 5. IC₅₀ Values (μmol/L) for compounds against Hela and Hep-G2 cells.

Compound	Toxicities (IC ₅₀ , μmol/L)	
	Hela (48 h)	Hep-G2 (48 h)
Cis-platin	11.73±0.99	12.97±0.98
Mitomycin	20.85±0.97	19.73±0.99
Ligand 1	1583.77±10.19	1949.28±7.53
Ligand 2	1375.75±10.73	1684.07±5.85
Complex 1	57.39±2.67	63.95±3.15
Complex 2	73.45±2.77	91.75±3.00

4. Conclusion

The reported work is concerned with the synthesis, crystal structure and *in vitro* anticancer studies of two bis(8-quinolinolato-N,O)-platinum(II) complexes. Both C₁₈H₁₂N₂O₂Pt (**1**) and C₂₀H₁₆N₂O₂Pt (**2**) crystallized in monoclinic crystal system. Intermolecular C–H···O hydrogen bonding interactions, as well as Pt···Pt and π–π stacking interactions, help to stabilize the crystal structures of complexes **1** and **2**. The preliminary *in vitro* anticancer activity of complexes **1** and **2** and the corresponding ligands (**L1** and **L2**) were investigated using human cervical (Hela) and hepatocellular carcinoma (Hep-G2) cancer cell lines. The platinum(II) complexes can greatly inhibit the cell proliferation and show stronger cytotoxic activities against the tested cancer cell lines than both ligands.

Acknowledgements

The authors acknowledge the Analytical & Testing Center of China Three Gorges University for CCD X-ray single crystal diffractometer work. The authors are also grateful to Dr. Daichuan Ma for help with the single crystal measurements. The authors would like to thank the Institute of Nuclear Science and Technology, Sichuan University for the first-principles DFT calculations of five Pt(II) complexes by using the Vienna ab-initio simulation package (VASP 5.2.2). The authors also thank Dr. Jianchun Wu, Dr. Yu Zou and Dr. Huan Wang for valuable discussions and for the help on the electronic structures calculations.

Supporting information

CCDC 1042740 and 1042741 contain the supplementary crystallographic data for this paper. These data can be obtained free of charge via <https://www.ccdc.cam.ac.uk/structures/>, or by e-mailing data_request@ccdc.cam.ac.uk, or by contacting The Cambridge Crystallographic Data Centre, 122 Union Road, Cambridge CB2 1EZ, UK; fax: +44(0)1223-336033.

Disclosure statement

Conflict of interests: The authors declare that they have no conflict of interest.

Author contributions: All authors contributed equally to this work.

Ethical approval: All ethical guidelines have been adhered.

Sample availability: Samples of the compounds are available from the author.

ORCID

Hong Chen

 <http://orcid.org/0000-0002-8415-7333>

Mingguo Liu

 <http://orcid.org/0000-0003-2686-3034>

References

- [1] Shi, X. C.; Chen, Z. Y.; Wang, Y. J.; Guo, Z. J.; Wang, X. Y. *Dalton Trans.* **2018**, 47, 5049-5054.
- [2] Hannon, M. J. *Chem. Soc. Rev.* **2007**, 36, 280-295.
- [3] Dyson, P. J.; Sava, G. *Dalton Trans.* **2006**, 1929-1933.
- [4] Guo, Z. J.; Sadler, P. J. *Adv. Inorg. Chem.* **2000**, 49, 183-306.
- [5] Zhang, S. R.; Yuan, H.; Guo, Y.; Wang, K.; Wang, X. Y.; Guo, Z. J. *Chem. Commun.* **2018**, 54, 11717-11720.
- [6] Kelland, L. *Nat. Rev. Cancer* **2007**, 7, 573-584.
- [7] Hannon M. J. *Pure Appl. Chem.* **2007**, 79, 2243-2261.
- [8] Fricker, S. P. *Dalton Trans.* **2007**, 4903-4917.
- [9] Reedijk, J. *Chem. Commun.* **1996**, 801-813.
- [10] Florea, A. M.; Büsselberg, D. *Cancers* **2011**, 3, 1351-1371.
- [11] Wang, X. Y.; Guo, Z. J. *Dalton Trans.* **2008**, 1521-1532.
- [12] Roberts, J. D.; Peroutka, J.; Farrell, N. J. *Inorg. Biochem.* **1999**, 77, 51-57.
- [13] Farrer, N. J.; Woods, J. A.; Salassa, L.; Zhao, Y.; Robinson, K. S.; Clarkson, G.; Mackay, F. S.; Sadler, P. J. *Angew. Chem. Int. Ed.* **2010**, 49, 8905-8908.
- [14] Miodragovic, D. U.; Quentzel, J. A.; Kurutz, J. W.; Stern, C. L.; Ahn, R. W.; Kandela, I.; Mazar, A.; O'Halloran, T. V. *Angew. Chem. Int. Ed.* **2013**, 52, 10749-10752.
- [15] Rosenberg, B.; VanCamp, L.; Trosko, J. E.; Mansour, V. H. *Nature* **1969**, 222, 385-386.
- [16] Reedijk, J. *Eur. J. Inorg. Chem.* **2009**, 2009, 1303-1312.
- [17] Wheate, N. J.; Walker, S.; Craig, G. E.; Oun, R. *Dalton Trans.* **2010**, 39, 8113-8127.
- [18] Wang, X. Y.; Guo, Z. J. *Chem. Soc. Rev.* **2013**, 42, 202-224.
- [19] Zhu, Z. Z.; Wang, X. Y.; Li, T. J.; Aime, S.; Sadler, P. J.; Guo, Z. J. *Angew. Chem. Int. Ed.* **2014**, 53, 13225-13228.
- [20] Wang, J. Z.; Wang, X. Y.; Song, Y. J.; Wang, J.; Zhang, C. L.; Chang, C. J.; Yan, J.; Qiu, L.; Wu, M. M.; Guo, Z. J. *Chem. Sci.* **2013**, 4, 2605-2612.
- [21] Varbanov, H. P.; Jakupec, M. A.; Roller, A.; Jensen, F.; Galanski, M.; Keppler, B. K. *J. Med. Chem.* **2013**, 56, 330-344.
- [22] Pichler, V.; Heffeter, P.; Valiahi, S. M.; Kowol, C. R.; Egger, A.; Berger, W.; Jakupec, M. A.; Galanski, M.; Keppler, B. K. *J. Med. Chem.* **2012**, 55, 11052-11061.
- [23] Liu, Z. P.; He, W. J.; Guo, Z. J. *Chem. Soc. Rev.* **2013**, 42, 1568-1600.
- [24] Tu, C.; Lin, J.; Shao, Y.; Guo, Z. J. *Inorg. Chem.* **2003**, 42, 5795-5797.
- [25] Proetto, M.; Liu, W. K.; Hagenbach, A.; Abram, U.; Gust, R. *Eur. J. Med. Chem.* **2012**, 53, 168-175.
- [26] Zhang, Q. Y.; Huang, N. Y.; Wang, J. Z.; Luo, H. J.; He, H. B.; Ding, M. R.; Deng, W. Q.; Zou, K. *Fitoterapia* **2013**, 89, 210-217.
- [27] Fang, H. B.; Jin, L.; Huang, N. Y.; Wang, J. Z.; Zou, K.; Luo, Z. G. *Chin. J. Chem.* **2013**, 31, 831-836.
- [28] Huang, N. Y.; Chen, L.; Liao, Z. J.; Fang, H. B.; Wang, J. Z.; Zou, K. *Chin. J. Chem.* **2012**, 30, 71-76.
- [29] Ballardini, R.; Varani, G.; Indelli, M. T.; Scandola, F. *Inorg. Chem.* **1986**, 25, 3858-3865.
- [30] Ballardini, R.; Indelli, M. T.; Varani, G.; Bignozzi, C. A.; Scandola, F. *Inorg. Chim. Acta* **1978**, 31, L423-L424.
- [31] Dolomanov, O. V.; Bourhis, L. J.; Gildea, R. J.; Howard, J. A. K. & Puschmann, H. *J. Appl. Cryst.* **2009**, 42, 339-341.
- [32] Sheldrick, G. M. A short history of SHELX. *Acta Cryst. A* **2008**, 64, 112-122.
- [33] Shapira, A.; Davidson, I.; Avni, N.; Assaraf, Y. G.; Livney, Y. D. *Eur. J. Pharm. Biopharm.* **2012**, 80, 298-305.
- [34] Etaiw, S. E. D. H.; Sultan, A. S.; El-Bendary, M. M. *J. Organomet. Chem.* **2011**, 696, 1668-1676.
- [35] Creaven, B. S.; Duff, B.; Egan, D. A.; Kavanagh, K.; Rosair, G.; Thangella, V. R.; Walsh, M. *Inorg. Chim. Acta* **2010**, 363, 4048-4058.
- [36] Chan, M. H. E.; Crouse, K. A.; Tahir, M. I. M.; Rosli, R.; Umar-Tsafe, N.; Cowley, A. R. *Polyhedron* **2008**, 27, 1141-1149.
- [37] Mosmann, T. *J. Immunol. Methods* **1983**, 65, 55-63.
- [38] Wu, H. L.; Yuan, J. K.; Pan, G. L.; Zhang, Y. H.; Wang, X. L.; Shi, F. R.; Fan, X. Y. *J. Photoch. Photobio. B* **2013**, 122, 37-44.
- [39] Kaniskan, N.; Ogretir, C. *J. Mol. Struct.* **2002**, 584, 45-52.
- [40] Cumming, G.; Fidler, F.; Vaux, D. L. *J. Cell Biol.* **2007**, 177, 7-11.
- [41] West, B. T. *Eval. Health Prof.* **2009**, 32, 207-228.
- [42] Kresse, G.; Hafner, J. *Phys. Rev. B* **1993**, 47, 558-561.

- [43]. Kresse, G.; Hafner, J. *Phys. Rev. B* **1994**, *49*, 14251-14269.
- [44]. Kresse, G.; Furthmuller, J. *Phys. Rev. B* **1996**, *54*, 11169-11186.
- [45]. Perdew, J. P.; Burke, K.; Ernzerhof, M. *Phys. Rev. Lett.* **1996**, *77*, 3865-3868.
- [46]. Kresse, G.; Joubert, D. *Phys. Rev. B* **1999**, *59*, 1758-1775.
- [47]. Dudarev, S. L.; Botton, G. A.; Savrasov, S.Y.; Humphreys, C.J.; Sutton, A. P. *Phys. Rev. B* **1998**, *57*, 1505-1509.
- [48]. Kato, M.; Ogawa, Y.; Kozakai, M.; Sugimoto, Y. *Acta Crystallogr. C* **2002**, *58*, m147-m149.
- [49]. Low, K. H.; Xu, Z. X.; Xiang, H. F.; Chui, S. S. Y.; Roy, V. A. L.; Che, C. M. *Chem. Asian J.* **2011**, *6*, 3223-3229.
- [50]. Janiak, C. *J. Chem. Soc., Dalton Trans.* **2000**, 3885-3896.
- [51]. Orpen, A. G.; Brammer, L.; Allen, F. H.; Kennard, O.; Watson, D. G.; Taylor, R. *J. Chem. Soc. Dalton Trans. II* **1989**, S1-S83.
- [52]. Wong, E.; Giandomenico, C. M. *Chem. Rev.* **1999**, *99*, 2451-2466.
- [53]. Jamieson, E. R.; Lippard, S. J. *Chem. Rev.* **1999**, *99*, 2467-2498.
- [54]. Qin, Q. P.; Chen, Z. F.; Qin, J. L.; He, X. J.; Li, Y. L.; Liu, Y. C.; Huang, K. B.; Liang, H. *Eur. J. Med. Chem.*, **2015**, *92*, 302-313.



Copyright © 2019 by Authors. This work is published and licensed by Atlanta Publishing House LLC, Atlanta, GA, USA. The full terms of this license are available at <http://www.eurjchem.com/index.php/eurjchem/pages/view/terms> and incorporate the Creative Commons Attribution-Non Commercial (CC BY NC) (International, v4.0) License (<http://creativecommons.org/licenses/by-nc/4.0>). By accessing the work, you hereby accept the Terms. This is an open access article distributed under the terms and conditions of the CC BY NC License, which permits unrestricted non-commercial use, distribution, and reproduction in any medium, provided the original work is properly cited without any further permission from Atlanta Publishing House LLC (European Journal of Chemistry). No use, distribution or reproduction is permitted which does not comply with these terms. Permissions for commercial use of this work beyond the scope of the License (<http://www.eurjchem.com/index.php/eurjchem/pages/view/terms>) are administered by Atlanta Publishing House LLC (European Journal of Chemistry).